J Appl Electrochem (2008) 38:837–843
DOI 10.1007/s10800-008-9521-7

ORIGINAL PAPER

Electrocatalytic oxidation of ethanol on $Sn_{(1-x)}Ir_{(x)}O_2$ electrodes in acid medium

D. Profeti · K. Servat · F. Hahn · K. B. Kokoh · P. Olivi

Received: 17 October 2007 / Revised: 5 February 2008 / Accepted: 13 February 2008 / Published online: 27 February 2008

Abstract The electrochemical oxidation of ethanol at $Sn_{(1-x)}Ir_xO_2$ electrodes (with $x = 0.01$, 0.05, 0.1 and 0.3) was studied in 0.1 mol L^{-1} $HClO_4$ solution. Electrolysis experiments were carried out and the reaction products were analyzed by Liquid Chromatography. It was found that the amounts of the reaction products depended on the composition of the electrode. In situ infrared reflectance spectroscopy measurements were performed to identify the adsorbed intermediates and to postulate a reaction mechanism for ethanol electrooxidation on these electrode materials. As evidence, acetaldehyde and acetic acid were formed through a successive reaction process. Carbon dioxide was also identified as the end product, showing that the cleavage of the carbon–carbon bond occurred. These results indicate that the synthesized catalysts are able to lead to the total combustion of organic compounds. Analysis of the water bending band at different potentials illustrated its role at the electrode interface.

Keywords Ethanol · Electrocatalytic oxidation · In situ infrared reflectance spectroscopy · Reaction mechanism · Tin oxide electrodes

D. Profeti · P. Olivi (✉)
Departamento de Química da Faculdade de Filosofia, Ciências e Letras de Ribeirão Preto, Universidade de São Paulo, Av. Bandeirantes, 3900, 14040-901 Ribeirao Preto, SP, Brazil
e-mail: olivip@ffclrp.usp.br

K. Servat · F. Hahn · K. B. Kokoh
Equipe Electrocatalyse, UMR 6503, CNRS—Université de Poitiers, 40, Avenue du Recteur Pineau, 86022 Poitiers Cedex, France

1 Introduction

The ever-growing importance of the electrochemical oxidation of organic compounds in wastewater treatment is due to increasing concerning with the cleanliness of the environment [1]. Because of the complexity of wastewaters produced in different industries, it is advisable that a model molecule is chosen in order to investigate the electrocatalytic activities of electrode materials. Otherwise, ethanol can be used as a model molecule because it presents distinct mechanism routes which involve either the cleavage of the C–C bond, leading to complete ethanol oxidation to CO_2, or a parallel mechanism that can produce acetic acid or acetaldehyde [2]. Thus, evaluation of a catalyst activity can be performed by analyzing ethanol consumption and product formation, which enables one to investigate the catalyst ability to completely oxidize an organic molecule.

Metal oxide electrodes can be used in the oxidation of some organic molecules, such as phenols [3–5] and aldehydes [6–9], present in polluted water. Comninellis and de Battisti's model for organic species oxidation on oxide electrodes considers that the reaction can occur under conditions of simultaneous oxygen evolution and that the oxidation mechanism and the reaction products are affected by the nature of the electrode [10]. In this model, the anodic oxidation of organic compounds in acid medium can occur in two ways: via formation of higher metal oxides, (MO_{x+1}), on "active" electrodes (e.g. RuO_2 or IrO_2), or through formation of hydroxyl radicals on "non-active" electrodes (e.g. SnO_2 or PbO_2) presenting low oxidation states. The "active" electrodes are known to promote selective oxidation, whereas "non-active" electrodes lead to complete oxidation. Based on this information, SnO_2 is a promising candidate for anode material in the electrochemical treatment of wastewater

since it can promote the complete oxidation of organic substances. However, SnO_2 has poor stability at high anodic potentials and improvements must be made in order to make this material useful for this purpose. Improved SnO_2 lifetime can be achieved by using a second metal oxide in the catalyst composition, but it is important that this oxide does not change the reaction mechanism and does not alter the reaction products. In this sense, iridium oxide is an interesting candidate because of its high anodic stability [11–14]. Recently, $Sn_{(1-x)}Ir_{(x)}O_2$ electrodes were used in the bleaching of an acid dye [15] and in the degradation of tannery wastewater [16]. In both cases, the electrodes showed good catalytic activity and good stability. Nevertheless, a detailed study of the possibility of direct oxidation of organic species on the electrode surface was not carried out.

The aim of this work is to investigate the influence of the modification of SnO_2 by IrO_2 in the mechanism of ethanol electrooxidation, which was chosen as a model molecule. The reaction products formed during long-period electrolyses were analyzed by chromatography, and the adsorbed intermediates were identified by in situ infrared reflectance spectroscopy.

2 Experimental

Four different electrodes with general composition $Sn_{(1-x)}Ir_{(x)}O_2$ ($x = 0.01$, 0.05, 0.1 and 0.3) were prepared by thermal decomposition of precursor solutions. The Sn precursor solution was prepared by the polymeric precursor method [17], and the Ir solution was prepared by dissolution of iridium chloride (Aldrich) in HCl 1:1 (v/v) solution. The precursor solutions were mixed in an appropriate ratio, to obtain the desired composition. The final solution was applied onto both sides of a 2 cm^2 pre-treated Ti support [16] (for the electrodes used in the electrolysis) or onto a polished 8 mm-diameter Au disc (for FTIR experiments), by brushing. The brushed Ti plates were submitted to a temperature of 120 °C for 5 min and subsequently to thermal decomposition carried out at 550 °C for 5 min under oxygen atmosphere. The brushing and thermal treatments were repeated until a nominal oxide layer thickness of 2 μm was achieved. The Au discs were brushed 2 times and were then submitted to the same thermal treatment. Both types of electrode were submitted to a post-treatment at 550 °C under oxygen for 1 h. Details of the preparation and characterization of these electrodes in acid solution are described elsewhere [15–17]. The composition of oxide layers were analysed by EDX and the results confirmed that the overall composition is close to the nominal one.

Voltammetric experiments were carried out in a conventional three-electrode Pyrex electrochemical cell. The apparatus consisted of a waveform generator (Wenking Model VSG72, Bank Electronik), a potentiostat (Wenking Model LB81), and an X-Y recorder (Linseis LY 17100). The counter electrode was a vitreous carbon plate, and a reversible hydrogen electrode (RHE) was used as reference. The electrolysis equipment consisted of a potentiostat/galvanostat (Autolab EcoChemie model PGSTAT30) interfaced with a computer. Electrolysis was carried out using a constant current density of 20 mA cm^{-2}.

IR reflectance spectra were recorded on a Bruker IFS 66v spectrometer, which allowed to perform Single Potential Alteration Infrared Reflectance Spectroscopy (SPAIRS) experiments [18–21]. The reflectivities were recorded at 100 mV intervals during the first voltammetric scan, at a low sweep rate (1 mV s^{-1}). Each spectrum resulted from the co-addition of 128 interferograms. Data acquisition required 20 s i.e. over ca. 20 mV. Spectra were calculated as $-\Delta A = \Delta R/R = (RE2 - RE1)/RE1$, where the "reference" spectrum, RE1, was that recorded at 400 mV versus RHE. The sample compartment of the IR spectrometer was modified, to allow the beam to be reflected on the electrode surface with an incidence angle of 65°, after passing through the IR window (CaF_2) of a conventional thin layer spectroelectrochemical cell. The beam path was maintained under vacuum and a liquid N_2 cooled HgCdTe detector (Infrared Associates) was used.

The solutions were prepared from ultra-pure water (Millipore Milli-Q System), and Merck "Suprapur" reagents ($HClO_4$, ethanol, acetaldehyde, acetic acid, and Na_2CO_3). Before each experiment, the solutions were deaerated with nitrogen (U Quality from Air Liquide), and a nitrogen stream was maintained over the solution during the measurements. All the experiments were performed at room temperature (21 ± 1 °C).

3 Results and discussion

3.1 Voltammetric study

Cyclic voltammetry was carried out in 0.1 mol L^{-1} $HClO_4$ and in 0.1 mol L^{-1} H_2SO_4 solutions, to investigate catalyst activity toward ethanol electrooxidation. Typical cyclic voltammograms scans of various IrO_2-content electrodes in H_2SO_4 solution and in the presence of 1.0 and 0.1 mol L^{-1}.

The onset of ethanol oxidation starts at ca. 1.1 V versus RHE in all the voltammetric profiles. In the case of the 30% IrO_2-content electrode (Fig. 1d), no oxidation peak is visible in the investigated potential range, but an increase in current density is observed in the potential region of the O_2 evolution reaction (OER). This behaviour is in excellent agreement with previously published results [22, 23] which

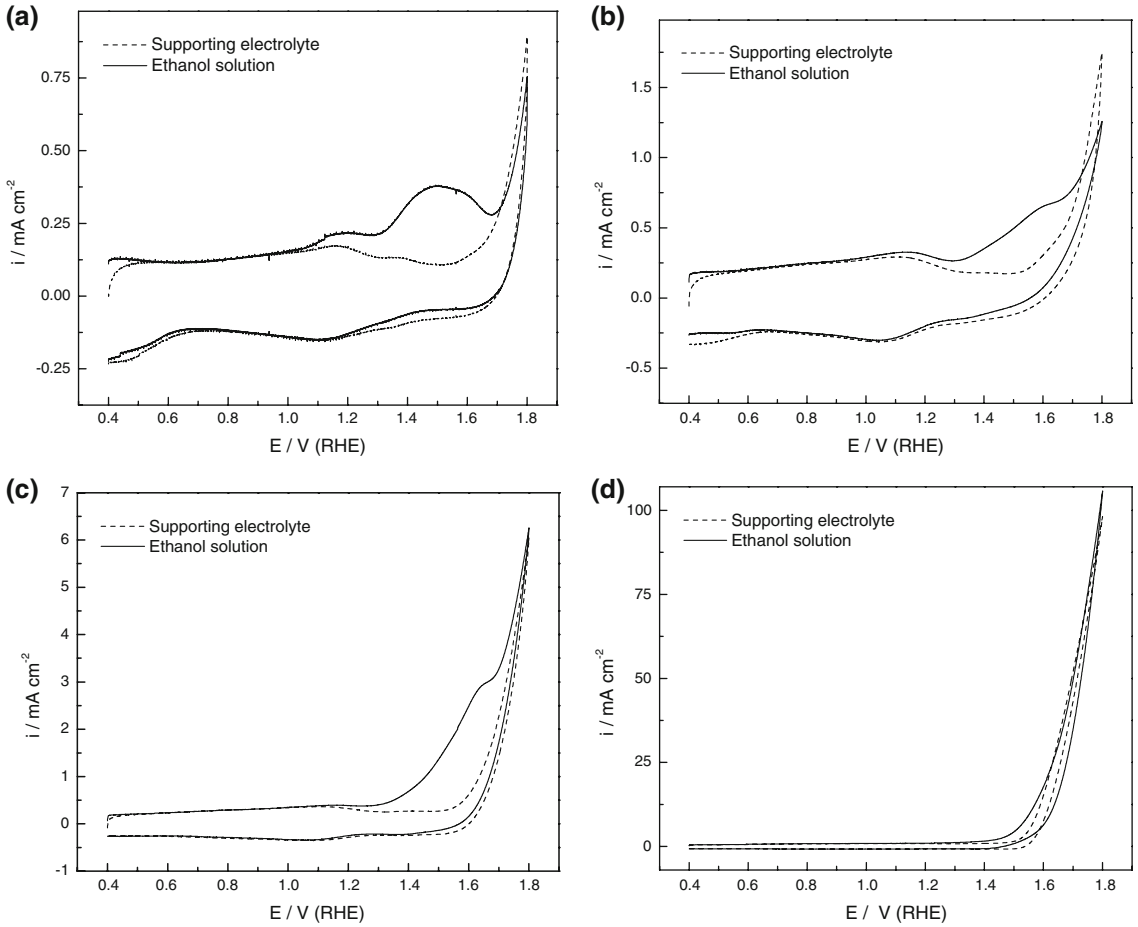

Fig. 1 Cyclic voltammograms of $Sn_{(1-x)}Ir_{(x)}O_2$ electrodes recorded at 20 mV s^{-1} in 0.1 mol L^{-1} H_2SO_4 supporting electrolyte alone and in the presence of 0.1 mol L^{-1} ethanol. $x = 0.01$ (**a**), 0.05 (**b**), 0.1 (**c**), and 0.3 (**d**)

showed that effective alcohol oxidation occurs simultaneously with the oxygen evolution reaction on $DSA^{(R)}$ type electrodes. IrO_2 is known as a good catalyst for OER and exhibits high performance when used as anode [24–26], and a competition between OER and ethanol electrooxidation can take place. All the electrode compositions exhibit the same voltammetric behaviour, but the increase in the amount of IrO_2 in the composition of the electrode material provokes an enhancement in the reactivity towards the OER. In these cases, the ethanol oxidation process becomes less evident.

3.2 Electrolysis

Long-term electrolyses experiments were carried out using a constant current of 20 mA cm^{-2} in a 15 mL volume solution, in order to verify the selectivity on $Sn_{(1-x)}Ir_xO_2$ electrodes. Analyses of the reaction products and the intermediates were performed by HPLC. The identified compounds were acetic acid (AA) and acetaldehyde (AAL), besides CO_2 in smaller amount. In Table 1, the conversion of ethanol and the selectivity of the reaction products formed on the $Sn_{(1-x)}Ir_xO_2$ electrodes after 4 h of electrolysis are given together with the ratio between the AAL and AA concentrations (AAL/AA).

The conversion yield (τ%) was calculated in the following way:

$$\tau(\%) = \frac{C_0 - C}{C_0} \times 100$$

Table 1 Analytical data obtained for each electrode composition after 4 h of electrolysis at 20 mA cm^{-2} in 0.1 mol L^{-1} $HClO_4$ and in the presence of 0.1 mol L^{-1} ethanol

Electrode (IrO_2 content)	1 (%)	5 (%)	10 (%)	30 (%)
Ethanol conversion (%)	5.6	4.8	7.1	5.7
AAL selectivity (%)	76.7	46.3	42.4	41.4
AA selectivity (%)	13.6	43.3	48.7	49.3
AAL/AA	5.6	1.1	0.9	0.8
CO_2 selectivity (%)	8.7	6.4	7.1	8.1

where C_0 is the substrate initial concentration; C is its remaining concentration at the end of electrolysis.

The selectivity of a reaction product S_x (%) is given by:

$$S_x(\%) = \frac{1}{v}\frac{C_x}{C_0 - C} \times 100$$

where C_x is the concentration of the reaction product at a given time, and v is the stoichiometric number.

It can be seen that the conversion of ethanol is similar for all the electrodes and reaches a maximum of ca. 7% when the Ir content is 10%. The selectivity toward acetaldehyde production decreases and the selectivity toward acetic acid increases with the increasing amount of Ir in the electrode composition. The largest difference is found for the electrode containing only 1 mol% of Ir. In this case, the AAL/AA ratio is more than 5 times higher than that obtained with the other electrodes. This shows that higher amounts of Ir at the electrode surface contribute to the oxidation of ethanol to acetic acid. CO_2 production, which occurs upon cleavage of the C–C bond, does not depend on the composition of the electrode material. Nevertheless, the AAL/AA ratio and the selectivity toward carbon dioxide confirm that higher IrO_2 contents promote acetic acid formation. Since a difference in the reaction mechanism may exist between IrO_2 and SnO_2, as pointed out by Comninellis et al. [10], in the presence of higher IrO_2 content in the electrode composition, ethanol electrooxidation must occur at the Ir sites preferentially, thus giving faster kinetics than the process occurring at the tin oxide sites. When a $Sn_{0.99}Ir_{0.01}O_2$ electrode composition is used, the main mechanism leads to preferential formation of acetaldehyde, and it must occur mainly on the SnO_2 sites. Additional electrolyses experiments with acetaldehyde (not shown) indicated that acetaldehyde can be oxidized with up to 100% consumption, being CO_2 formed in yields higher than 50%, and acetic acid can also be detected depending on the electrode composition. It is known that it is difficult to oxidize acetic acid and its formation must be avoided. In this context, the present results indicate that the use of the electrode containing 1% Ir can lead to better results than the electrodes containing more Ir in their composition since the former produces less acetic acid and more acetaldehyde, which can be later oxidized to CO_2, thus increasing the overall yield of organic degradation.

3.3 SPAIR spectroscopic study

The IR spectra recorded for different catalysts in a 0.1 mol L^{-1} $HClO_4$ + CH_3CH_2OH solution are shown in Figs. 2–5. The most important feature in Fig. 2 is the absorption band at around 1,650 cm^{-1}, which is ascribed to the δ_{HOH} deformation mode of the interfacial water. This band, which is due to the activation of H_2O molecules, is more visible at high Sn content in the catalyst. This can be explained by the accumulation of the OH groups at the interface which furnishes $Sn(OH)_2$ and/or SnO_2 species [30]. However, the water molecules interact with the electrode surface and thus compete with ethanol molecules. This is in agreement with the voltammetric results (Fig. 1), where no traces of ethanol are noticed at concentrations lower than 0.1 mol L^{-1}.

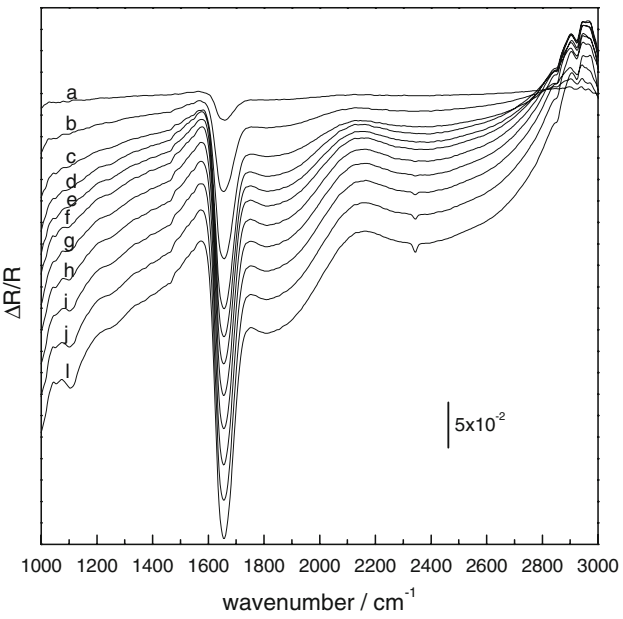

Fig. 2 SPAIR spectra recorded from 0.1 mol L^{-1} ethanol in 0.1 mol L^{-1} $HClO_4$ on 1 mol% IrO_2 electrode at various potentials (top to bottom: (a) 500, (b) 700, (c) 900, (d) 1,100, (e) 1,200, (f) 1,300, (g) 1,400, (h) 1,500, (i) 1,600, (j) 1,700 and (l) 1,800 mV versus RHE), $R_{E\ \mathrm{Ref}}$ taken at 400 mV versus RHE

Figures 3 and 4 clearly show that the band centered at 1,650 cm^{-1} splits into two peaks (1,650 and 1,717 cm^{-1}), thereby indicating the contribution of a reaction product such as acetaldehyde and/or acetic acid. The latter product is most likely at higher potentials because its presence is often concomitant with those peaks at 1,280 and 2,616 cm^{-1} which are characteristic of acetic acid [27–29]. As can be seen in the spectra (Figs. 3–5), the band due to CO_2 appears at 2,345 cm^{-1} without the presence of the CO band (at around 2,050 cm^{-1}). This may be explained by the high potentials applied in this work. In fact, at potential values higher than 0.7 V versus RHE CO rapidly reacts with tin oxides/hydroxides at the electrode surface to form carbon dioxide, which immediately diffuses into solution [33, 34]. As for the electrode containing 10% IrO_2, the band was observed from 1.2 V (Fig. 6) while for other compositions from 1.3 V. This confirms that the C–C bond cleavage occurs in those electrodes.

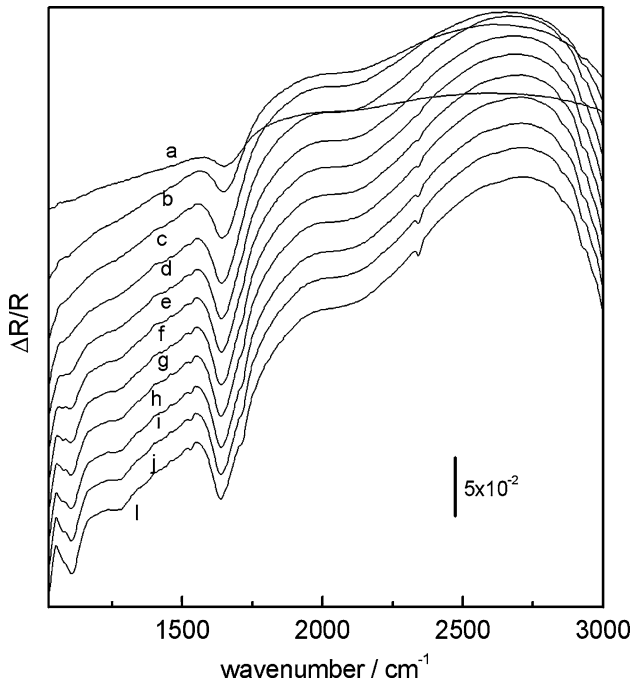

Fig. 3 SPAIR spectra recorded from 0.1 mol L^{-1} ethanol in 0.1 mol L^{-1} $HClO_4$ on 5mol% IrO_2 electrode at various potentials (top to bottom: (a) 500, (b) 700, (c) 900, (d) 1,100, (e) 1,200, (f) 1,300, (g) 1,400, (h) 1,500, (i) 1,600, (j) 1,700 and (l) 1,800 mV versus RHE), $R_{E\ \mathrm{Ref}}$ taken at 400 mV versus RHE

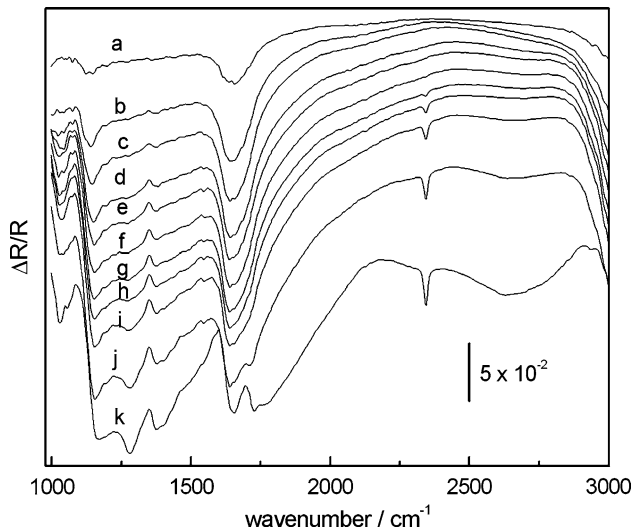

Fig. 4 SPAIR spectra recorded from 0.1 mol L^{-1} ethanol in 0.1 mol L^{-1} $HClO_4$ on 10 mol% IrO_2 electrode at various potentials (top to bottom: (a) 500, (b) 700, (c) 900, (d) 1,100, (e) 1,200, (f) 1,300, (g) 1,400, (h) 1,500, (i) 1,600, (j) 1,700 and (l) 1,800 mV versus RHE), $R_{E\ \mathrm{Ref}}$ taken at 400 mV versus RHE

The spectra in Fig. 5 also show the 3,000–4,000 cm^{-1} spectral range, where it is possible to observe a positive and broad band between 3,000 and 3,600 cm^{-1} corresponding to the water stretching vibrations. These observations agree

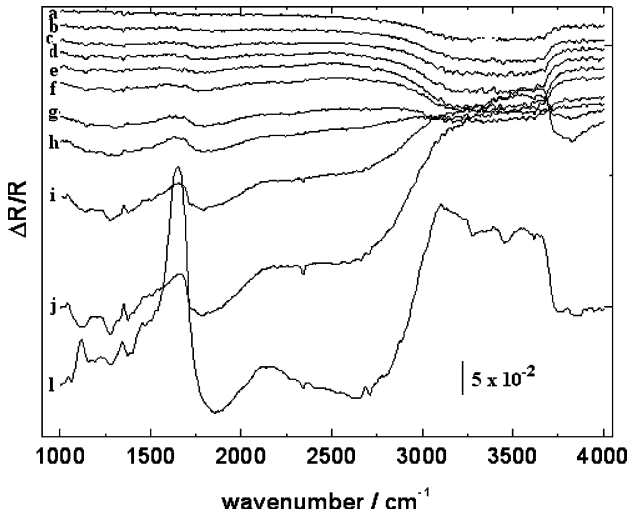

Fig. 5 SPAIR spectra recorded from 0.1 mol L^{-1} ethanol in 0.1 mol L^{-1} $HClO_4$ on 30 mol% IrO_2 electrode at various potentials (top to bottom: (a) 500, (b) 700, (c) 900, (d) 1,100, (e) 1,200, (f) 1,300, (g) 1,400, (h) 1,500, (i) 1,600, (j) 1,700 and (l) 1,800 mV versus RHE), $R_{E\ \mathrm{Ref}}$ taken at 400 mV versus RHE

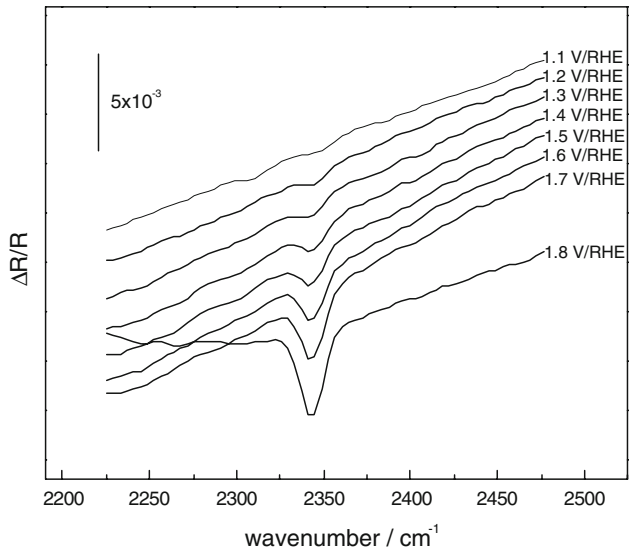

Fig. 6 SPAIR spectra recorded from 0.1 mol L^{-1} ethanol in 0.1 mol L^{-1} $HClO_4$ on 10 mol% IrO_2 electrode at potentials from 1,100 to 1,800 mV (detail of Fig. 4 extracted at CO_2 absorption band region), $R_{E\ \mathrm{Ref}}$ taken at 400 mV versus RHE

with the behaviour observed for the water bending band in the 1,650 cm^{-1} range and confirms the water consumption at the electrode surface. The process associated with water consumption is the oxygen evolution reaction (OER), and this observation is in agreement with the behaviour observed by cyclic voltammetry in supporting electrolyte solutions. In the voltammetric experiments, the OER begins at lower potentials for electrodes containing higher Ir content than the electrodes richer in Sn. The behaviour of water bands allow us to conclude that electrodes containing higher

amount of SnO_2 favour the formation of "interfacial water", which is able to displace ethanol from the electrode surface. In these electrodes, the OER shifts to lower potential values compared with electrodes containing higher amounts of IrO_2.

For all the electrode compositions, it is difficult to ascribe the carbonyl band for a carboxylic group or to an aldehyde group because they are separated by ca. 5 cm^{-1}, while the IR set-up resolution is 4 cm^{-1}. However, the bands located between 1,280 and 1,400 cm^{-1} can help discriminate between acetic acid and acetaldehyde. The bands in the 1,375–1,390 cm^{-1} range and those around 1,280 cm^{-1}, assigned to $\delta(CH_3)$ and ν(C–O), respectively, are absent in the spectrum of aqueous acetaldehyde, but present in that of aqueous acetic acid [29–33]. In this way, the acetaldehyde formation can be deduced indirectly. In Figs. 4 and 5, with 10 and 30 % IrO_2 content electrodes, respectively, acetaldehyde is formed first (see the carbonyl band from 700 mV), and then the band for acetic acid starts appearing at 1,000 mV, i.e. at 300 mV more positive potential. However, for the $Sn_{0.99}Ir_{0.01}O_2$ and $Sn_{0.95}Ir_{0.05}O_2$ compositions, the band associated with interfacial water hides that of the carbonyl, despite acetaldehyde and acetic acid having been detected in solution by HPLC during the electrolysis experiments on these electrode compositions.

The positive band close to 1,050 cm^{-1} is associated with a C–O stretching mode related to ethanol consumption. Other bands can be seen at about 2,950 cm^{-1} and at around 1,111 cm^{-1}, which are due to the ν(CH) of CH_3 and the Cl–O stretching of perchlorate anions, respectively [32].

3.4 Comparison between electrolysis and FTIR results during ethanol electrooxidation on $Sn_{(1-x)}Ir_xO_2$ electrodes

Results of the electrolysis on $Sn_{(1-x)}Ir_xO_2$ electrodes showed that ethanol was oxidized with simultaneous OER, and that AAL, AA and CO_2 were produced. Changes were only found in the yields of each product on the different electrodes. The lower Ir content presented higher efficiency for ethanol oxidation, with higher CO_2 production. As expected, the higher Sn content favoured CO_2 formation. These results were also confirmed also by SPAIR spectra obtained on $Sn_{(1-x)}Ir_xO_2$ electrodes during ethanol electrooxidation (Figs. 2–5), using the CO_2 band located at 2,345 cm^{-1} to monitor the reaction. For a better comparison, the intensity of the CO_2 IR band as function of potential is shown for all electrodes in Fig. 7. At higher potentials, the CO_2 band is more intense for 1% Ir content, followed by 30% Ir content. However, the band appears only at 1.4 V for 1% Ir content, whereas for 10% Ir content it appears from 1.2 V. Similar results were found for

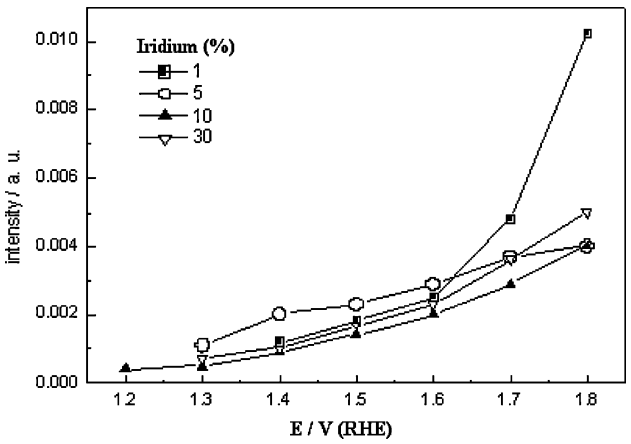

Fig. 7 Intensity of the CO_2 absorption band located close to 2,345 cm^{-1} drawn from Figs. 2–5 for the following IrO_2 contents in the electrode compositions: 1% (■), 5% (o), 10% (▲) and 30% (▽)

ethanol electrooxidation on gold [33]; i.e. CO_2 formation was observed at potentials higher than 1.15 V versus RHE, and adsorbed-CO species were not formed. However, in a quantitative comparison, the intensity of the CO_2 band at 1.75 V for the 1% Ir content electrode is around 5 times higher than that on gold under the same conditions. Otherwise, acetic acid is the main reaction product on 10 and 30% Ir contents electrodes (see Table 1). This result is in agreement with that obtained by SPAIRS, where the intensity of the band due to the ν(C–OH) mode at 1,280 cm^{-1} is higher for these two electrode compositions.

From both chromatographic and spectroscopic results we can postulate the following reaction mechanism for the different electrodes:

As shown in the Scheme 1, it can be assumed that acetic acid is formed from acetaldehyde through a process involving successive reactions, as observed in previous studies by DEMS [34] and infrared spectroscopy [35–39]. We have verified by electrolysis experiments (not shown) that the formed acetic acid remains in solution because it cannot be oxidized under the experimental conditions used in this work.

From these results, the distribution of the reaction products is dependent on the composition of the electrode material. CO_2 production is favoured on the electrode

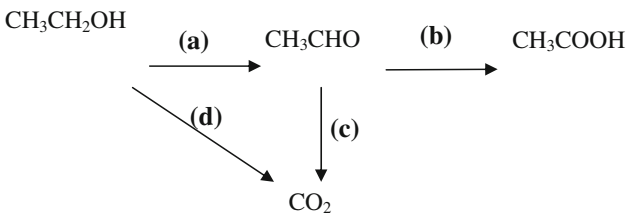

Scheme 1 General mechanism of ethanol electrooxidation on $Sn_{(1-x)}Ir_xO_2$ electrocatalysts

surface containing 1% IrO_2, due to the higher formation of $OH^{\bullet}_{ads}$ on electrodes richer in SnO_2.

4 Conclusion

Ethanol electrooxidation on $Sn_{(1-x)}Ir_xO_2$ electrodes was studied by in situ reflectance infrared spectroscopy coupled with long-term electrolysis. These complementary techniques show that the electrodes are able to promote the direct oxidation of ethanol. Acetaldehyde, acetic acid and CO_2 are the main electrooxidation products identified for all the electrode compositions. It is suggested that the reaction proceeds in a process involving successive reactions that can lead to complete ethanol oxidation to form CO_2 or to the formation of acetic acid as final products. A decreased amount of Ir oxide increases the amount of CO_2 formed, thus confirming that ethanol oxidation involves cleavage of the C–C bond. However, with increased IrO_2 content in the electrode, the selectivity toward acetic acid increased. In the case of the electrode containing 30% IrO_2 the high formation of acetic acid competes with the selectivity for CO_2. A higher concentration of "interfacial water" can also displace ethanol from the interface region on electrodes containing higher amounts of SnO_2.

Acknowledgements D. Profeti thanks the CAPES foundation and FAPESP, Brazil, for providing a travelling scholarship (Proc. BEX 0352/03-9) and Ph.D. scholarship in Brazil (Proc. 00/08734-3).

References

1. Foti G, Gandini D, Comninellis C, Perret A, Haenni W (1999) Electrochem Solid State Lett 2:228
2. Ribeiro J, dos Anjos D M, Kokoh K B, Coutanceau C, Léger J-M, de Andrade A R, Tremiliosi-Filho G (2007) Electrochim Acta 52:6997
3. Comninellis C, Nerini A (1995) J Appl Electrochem 25:23
4. Comninellis C, Pulgarin C (1993) J Appl Electrochem 23:108
5. Pelegrino RL, Di Iglia RA, Sanches CG, Avaca LA, Bertazzoli R (2002) J Braz Chem Soc 13:60
6. Motheo AJ, Gonzalez ER, Tremiliosi-Filho G, Olivi P, de Andrade AR, Kokoh B, Léger J-M, Belgsir EM, Lamy C (2000) J Braz Chem Soc 11:16
7. Malpass GRP, Motheo AJ (2001) J Appl Electrochem 31:1351
8. Malpass GRP, Motheo AJ (2003) J Braz Chem Soc 14:65
9. Motheo AJ, Tremiliosi-Filho G, Gonzalez ER, Kokoh KB, Léger J-M, Lamy C (2006) J Appl Electrochem 36:1035
10. Comninellis C, de Battisti A (1996) J Chim Phys 93:673
11. Birss VI, Andreas H, Serebrennikova I, Elzanowska H (1999) Electrochem Solid State Lett 2:326
12. Tsaprailis H, Birss VI (2004) Electrochem Solid State Lett 7:A348
13. Liao S, Holmes KA, Tsaprailis H, Birss VI (2006) J Am Chem Soc 128:504
14. Sivakumar P, Tricoli V (2006) Electrochem Solid State Lett 9:A167
15. Oliveira FH, Osugi ME, Paschoal FMM, Profeti D, Olivi P, Zanoni MVB (2007) J Appl Electrochem 37:583
16. Costa CR, Botta CMR, Espindola ELG, Olivi P (2008) Electrochemical treatment of tannery wastewater using DSA® electrodes, J Hazard Mat (in press), doi: 10.1016/j.jhazmat.2007.09.005
17. Rodrigues ECPE, Olivi P (2003) J Phys Chem Solids 64:1105
18. Corrigan DS, Leung LWH, Weaver MJ (1987) Anal Chem 59:2252
19. Corrigan DS, Weaver MJ (1988) J Electroanal Chem 241:143
20. Druliolle H, Kokoh KB, Hahn F, Lamy C, Beden B, (1997) J Electroanal Chem 426:103
21. Sun S-G (1998) In: Lipkowski J, Ross PhN (eds) Electrocatalysis, Frontiers in Electrochemistry, Wiley-VCH, New York, p 243
22. Simond O, Schaller V, Comninellis C (1997) Electrochim Acta 42:2009
23. Simond O, Comninellis C (1997) Electrochim Acta 42:2013
24. Trasatti S (1981) Electrodes of conductive metallic oxides. Elsevier, Amsterdam
25. Vercesi GP, Salamin J-Y, Comninellis C (1991) Electrochim Acta 36:991
26. De Pauli CP, Trasatti S (1995) J Electroanal Chem 396:161
27. Simões FC, dos Anjos DM, Vigier F, Léger J-M, Hahn F, Coutanceau C, Gonzalez ER, Tremiliosi-Filho G, de Andrade AR, Olivi P, Kokoh KB (2007) J Power Sources 167:1
28. Kokoh KB, Hahn F, Belgsir EM, Lamy C, de Andrade AR, Olivi P, Motheo AJ, Tremiliosi-Filho G (2004) Electrochim Acta 49:2077
29. dos Anjos DM, Hahn F, Léger J-M, Kokoh KB, Tremiliosi-Filho G (2007) J Solid State Electrochem 11:1567
30. Perez JM, Beden B, Hahn F, Aldaz A, Lamy C (1989) J Electroanal Chem 262:251
31. de Tacconi NR, Lezna RO, Beden B, Hahn F, Lamy C (1994) J Electroanal Chem 379:329
32. Iwasita T, Rasch B, Cattaneo E, Vielstich W (1989) Electrochim Acta 34:1073
33. Tremiliosi-Filho G, Gonzalez ER, Motheo AJ, Belgsir EM, Léger J-M, Lamy C (1998) J Electroanal Chem 444:31
34. Méndez E, Rodríguez JL, Arévalo MC, Pastor E (2002) Langmuir 18:763
35. Iwasita T, Pastor E (1994) Electrochim Acta 39:531
36. De Souza JPI, Queiroz SL, Bergamaski K, Gonzalez ER, Nart FC (2002) J Phys Chem B 106:9825
37. Lamy C, Rousseau S, Belgsir EM, Coutanceau C, Léger J-M (2004) Electrochim Acta 49:3901
38. Vigier F, Coutanceau C, Hahn F, Belgsir EM, Lamy C (2004) J Electroanal Chem 563:81
39. Vigier F, Coutanceau C, Perrard A, Belgsir EM, Lamy C (2004) J Appl Electrochem 34:439